JACS
JOURNAL OF THE AMERICAN CHEMICAL SOCIETY
Article
pubs.acs.org/JACS

A General Decomposition Pathway for Phosphine-Stabilized Metathesis Catalysts: Lewis Donors Accelerate Methylidene Abstraction

William L. McClennan, Stephanie A. Rufh, Justin A. M. Lummiss, and Deryn E. Fogg*

Department of Chemistry and Centre for Catalysis Research & Innovation, University of Ottawa, Ottawa, Ontario K1N 6N5, Canada

Supporting Information

ABSTRACT: Sterically accessible Lewis donors are shown to accelerate decomposition during catalysis, for a broad range of Grubbs-class metathesis catalysts. These include benzylidene derivatives $RuCl_2(NHC)(PCy_3)(=CHPh)$ (**Ru-2**: NHC = H_2IMes, **a**; IMes, **b**; H_2IPr, **c**; IPr, **d**; H_2ITol, **e**) and indenylidene complexes $RuCl_2(NHC)(PCy_3)(=C_{15}H_{10})$ (NHC = H_2IMes, **Ru-2f**; IMes, **Ru-2g**). All of these precatalysts form methylidene complex $RuCl_2(NHC)(=CH_2)$ **Ru-3** as the active species in metathesis of terminal olefins, and generate $RuCl_2(NHC)(PCy_3)(=CH_2)$ **Ru-4** as the catalyst resting state. On treatment with a 10-fold excess of pyridine, **Ru-4a** and **Ru-4b** decomposed within minutes in solution at RT, eliminating $[MePCy_3]Cl$ **A** by net loss of three ligands (PCy_3, methylidene, and one chloride), and a mesityl proton. In comparison, loss of **A** from **Ru-4a** in the absence of a donor requires up to 3 days at 55 °C. The σ-alkyl intermediate $RuCl_2(^{13}CH_2PCy_3)(NHC)(py)_2$ resulting from nucleophilic attack of free PCy_3 on the methylidene ligand was undetectable for the H_2IMes system, but was spectroscopically observable for the IMes system. The relevance of this pathway to decomposition of catalysts **Ru-2a–g** was demonstrated by assessing the impact of pyridine on the in situ-generated methylidene species. Slow initiation (as observed for the indenylidene catalysts) did not protect against methylidene abstraction. Importantly, studies with **Ru-4a** and **Ru-4b** indicated that weaker donors (THF, MeCN, DMSO, MeOH, and even H_2O) likewise promote this pathway, at rates that increase with donor concentration, and severely degrade catalyst productivity in RCM, even for a readily cyclized substrate. In all cases, **A** was the sole or major ^{31}P-containing decomposition product. For DMSO, a first-order dependence of decomposition rates on DMSO concentration was established. This behavior sends a warning about the use of phosphine-stabilized metathesis catalysts in donor solvents, or with substrates bearing readily accessible donor sites. Addition of pyridine to $RuCl_2(H_2IMes)(PCy_3)(=CHMe)$ did not result in ethylidene abstraction, indicating that this decomposition pathway can be inhibited by use of substrates in which the olefin bears a β-methyl group.

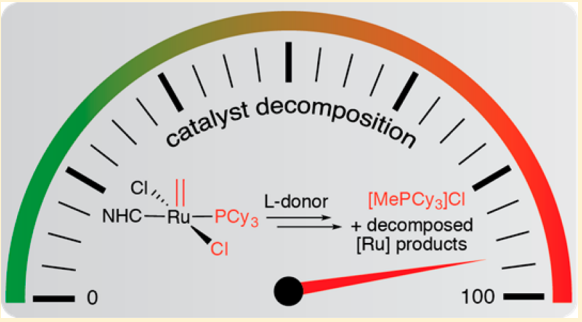

INTRODUCTION

Molecular metathesis catalysts have transformed organic synthesis in academia.[1,2] With pharmaceutical and specialty-chemicals manufacturing processes now emerging,[3−6] the demand for improved understanding of catalyst decomposition is increasing.[7,8] Catalyst lifetimes control metathesis productivity, and are also critical to product selectivity, because decomposed catalyst species can catalyze side-reactions such as C=C isomerization.[9,10] A central question is therefore the nature of the decomposition pathways operative during catalysis.[7,8] Examined here is the decomposition of phosphine-stabilized catalysts (Chart 1) by Lewis donors. Such donors may be present as unprotected functional groups on substrates or solvents, or as contaminants introduced with the solvent, a reagent, or prior synthetic steps.[9]

In the hundreds of ruthenium metathesis catalysts developed to date,[1,11] a recurring structural feature is a stabilizing phosphine ligand that is lost during initiation. Reaction of the liberated phosphine with $RuCl_2(NHC)(=CH_2)$ **Ru-3**, a key catalytic intermediate formed in metathesis of terminal olefins, generates the catalyst resting state **Ru-4** (Scheme 1, top). The

Chart 1. Metathesis Catalysts Examined[a]

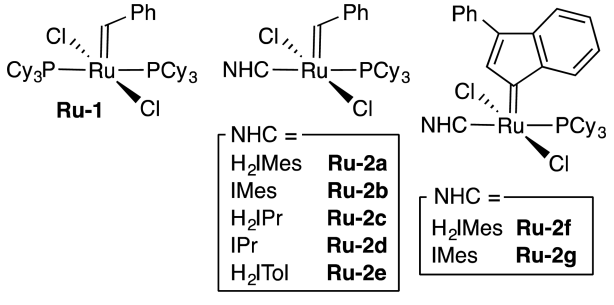

[a]For the structures of the NHC ligands, see Figure S1.

Received: August 12, 2016
Published: October 13, 2016

DOI: 10.1021/jacs.6b08372
J. Am. Chem. Soc. 2016, 138, 14668−14677

Scheme 1. Reactions of Ru-3 with Free PCy_3: Phosphine Reuptake vs Methylidene Abstraction

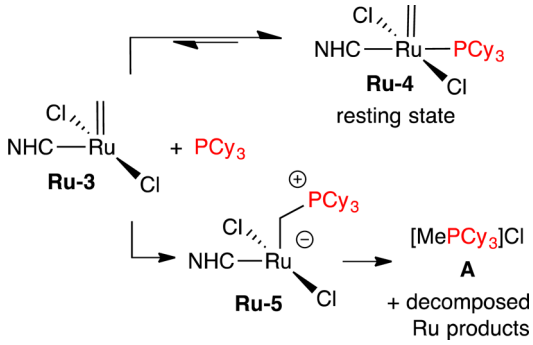

latter species is slow to re-enter the active cycle,[12] owing to the inverse trans effect exerted by the NHC ligand,[13] and the limited steric pressure exerted by the methylidene moiety, relative to the benzylidene group in the precatalyst.[14,15]

An alternative, more deleterious reaction pathway (Scheme 1, bottom) has been established[13,16] for the H_2IMes derivative **Ru-3a**. Here nucleophilic attack by free PCy_3 on the methylidene carbon[17] culminates in release of $[MePCy_3]Cl$ **A**: that is, in loss of three ligands (methylidene, phosphine, and one chloride ligand, as well as a proton). This catalyst decomposition pathway, originally described as requiring 3 days at 55 °C,[16,18] was found to occur much more rapidly on coordination of amines.[19−21] In the present work, we demonstrate that "donor-accelerated decomposition" is general for phosphine-stabilized catalysts of the Grubbs class, including indenylidene catalysts, and that it is promoted by a range of weaker donors, including MeCN, DMSO, H_2O, THF, and methanol. We show that the mechanism is associative in donor, and that the rate of decomposition therefore increases with increasing concentration. Finally, we demonstrate that the ethylidene complex $RuCl_2(H_2IMes)(PCy_3)(=CHMe)$ does not undergo alkylidene abstraction by PCy_3. Collectively, these findings have important implications for use of the large class of ruthenium metathesis catalysts based on the archetypal, phosphine-stabilized Grubbs catalyst **Ru-2a**.

RESULTS AND DISCUSSION

Observation of the σ-Alkyl Intermediate in the Second-Generation System. In a prior communication,[20] we described the near-quantitative formation and crystallographic characterization of a σ-alkyl intermediate (**Ru-7**, Scheme 2) generated by reaction of the first-generation Grubbs methylidene complex **Ru-6** with pyridine. In this system, *both* PCy_3 ligands were displaced by pyridine. In consequence, elimination of the alkyl ligand took place only over days in solution at RT, or 18 h at 60 °C. ^{13}C-Labeling studies enabled location of the diagnostic $^{13}C\{^1H\}$ NMR doublet for the $Ru-^{13}CH_2PCy_3$ moiety, which appears unusually far upfield (δ_C −12.3 ppm; $^1J_{PC}$ = 9.8 Hz) owing to shielding of the carbon nucleus by the formally anionic Ru center. The ^{31}P nucleus is correspondingly deshielded by its positive charge, and the $^{31}P\{^1H\}$ NMR doublet for ***Ru-7** is shifted ca. 20 ppm downfield relative to the value for **Ru-6**, to 55.7 ppm.

Under the same conditions, the labeled H_2IMes complex **Ru-4a** decomposed within minutes (87% ***A**, 13% free PCy_3), without observable intermediates. We hypothesized that a σ-alkyl intermediate is formed, but that it is very short-lived,

Scheme 2. Intercepted σ-Alkylphosphonium Species

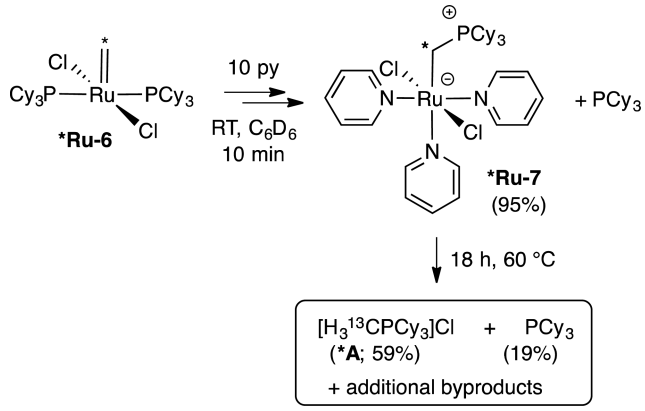

because facile C−H activation of the mesityl *o*-methyl groups promotes the elimination step. Such C−H activation is a common feature for the H_2IMes and IMes ligands.[22] For H_2IMes complexes, this susceptibility may be enhanced by the significant double-bond character present in the Ru−H_2IMes bond, a consequence of π-back-donation from Ru onto the saturated Arduengo carbene.[23] Backbonding has been shown to retard rotation about the Ru−H_2IMes bond in **Ru-4a**.[13] The corresponding σ-alkyl intermediate **Ru-8a** may thus be locked into a conformation that favors the incipient interaction between the σ-alkyl carbon and the mesityl group,[24,25] upon swivelling about the N−C_{Mes} bond (Chart 2a and inset).[26,27]

Chart 2. Ru−NHC Rotation in Second-Generation σ-Alkyl Species, and Impact on C−H Activation (Inset)

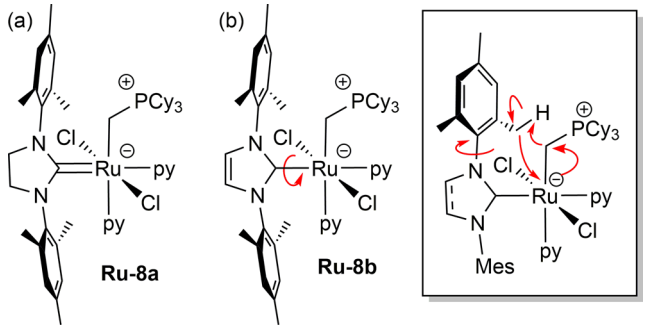

In seeking evidence for such a σ-alkyl intermediate in the second-generation systems, we turned to the "unlocked" complex **Ru-8b** (Chart 2b), in which we anticipated that free rotation of the IMes ligand should retard C−H activation. A ^{31}P NMR signal was indeed observed at ca. 61 ppm immediately after adding 10 equiv pyridine to a C_6D_6 solution of **Ru-4b**, but elimination of phosphonium salt $[MePCy_3]Cl$ **A** was complete within 15 min. Injection of a smaller excess of pyridine (3 equiv) resulted in slower decomposition of **Ru-4b**: we will return to the mechanistic implications of this observation below. Under these conditions, **Ru-8b** decomposed at a rate slightly slower than the rate at which it formed (Figure 1). Thus, a singlet was observed at 61.3 ppm (maximum 13%), but was rapidly exceeded in intensity by the singlet due to **A** at 34.2 ppm. After 75 min, neither **Ru-4b** nor **Ru-8b** remained: the dominant ^{31}P-containing species was **A** (ca. 90%). A small proportion of free PCy_3 was also observed, indicating a minor contribution from an additional, unidentified pathway. Given

DOI: 10.1021/jacs.6b08372
J. Am. Chem. Soc. 2016, 138, 14668−14677

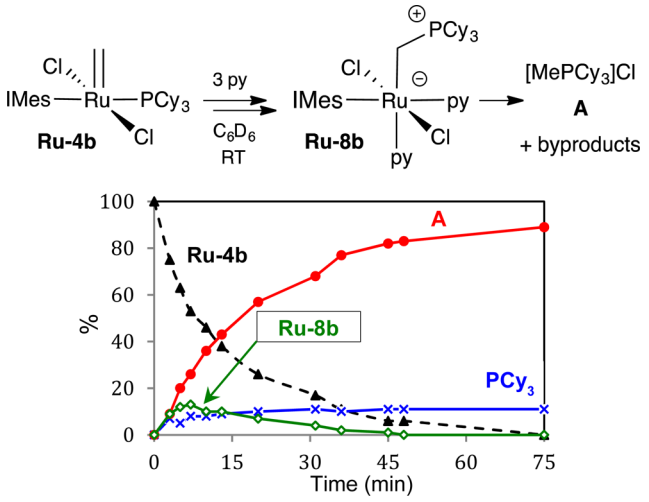

Figure 1. Direct observation of the short-lived σ-alkyl intermediate formed by IMes complex **Ru-4b** (20 mM [Ru], RT = 22 °C).

the transience and low concentration of putative **Ru-8b**, we turned to ^{13}C labeling studies for unequivocal confirmation of its identity.

Accordingly, ^{13}C-labeled ***Ru-4b** was prepared by the method previously developed for its H_2IMes analogue ***Ru-4a**,[21] and treated with a 3-fold excess of pyridine at ambient temperature in C_6D_6. NMR analysis was initiated immediately after injecting pyridine. Diagnostic $^{13}C\{^1H\}$ and $^{31}P\{^1H\}$ NMR doublets for ***Ru-8b** were observed (δ_C −27.4 ppm, δ_P 61.3 ppm; $^1J_{PC}$ = 12 Hz). This multiplicity, and the magnitude of the J_{CP} coupling constant, offer strong evidence for the proposed assignment, comparing well with values for ***Ru-7** (Figure 2).

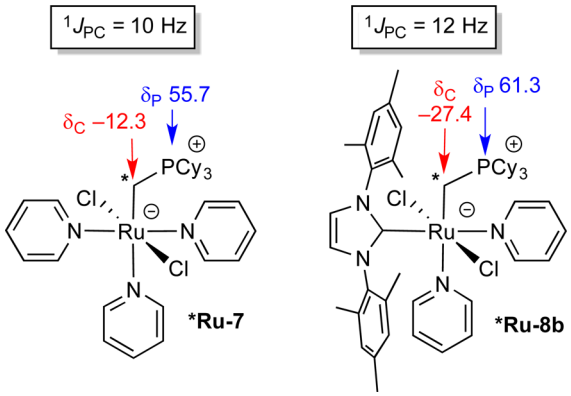

Figure 2. Key NMR shifts for first- and second-generation σ-alkyl complexes.

The location of the Ru−*C* signal in ***Ru-8b**, ca. 15 ppm further upfield than that for ***Ru-7**, is consistent with shielding by the more strongly donating[13,23] IMes ligand, relative to the pyridine ligands in ***Ru-7**. A six-coordinate, bis(pyridine) structure is shown, by analogy to that established crystallographically for **Ru-7**[20] and for the H_2IMes derivative of the benzylidene precatalyst.[28] However, all of these complexes are likely to exist in dynamic equilibrium with the five-coordinate monopyridine species.[29]

We conclude that the mechanism established for **Ru-6** is indeed also operative in the second-generation systems. That is: (1) the incoming donor displaces the PCy_3 ligand[30] and stabilizes the resulting methylidene species; (2) nucleophilic attack of the free phosphine on the methylidene carbon ensues, forming the σ-alkyl intermediate; and (3) the alkyl moiety is liberated as the phosphonium salt **A** by abstraction of a proton from the NHC ligand (confirmed by *d*-labeling studies, see below), as well as a chloride ligand. For sterically unencumbered amines of sufficiently high nucleophilicity, direct methylidene abstraction by amine has been shown to offer a competing pathway: $NH_2{}^nBu$, for example, abstracts the methylidene ligand as neutral $NHMe^nBu$.[19,21] No evidence of the corresponding methylpyridinium chloride was observed in the present work, however.

Scope with Respect to Catalyst. The broader relevance of this pathway was examined for an array of commercially available catalysts (**2a**−**2g**; Chart 1), upon metathesis with ethylene at 50 °C. This treatment generates the methylidene species **Ru-3**/ **Ru-4** in situ, enabling us to assess the impact of added pyridine on the proportion of $[MePCy_3]Cl$ **A** present at 2 h. In all cases, pyridine treatment accelerated catalyst decomposition, with the extent of of methylidene abstraction (as judged from % **A**) ranging from 80−100%: see Figure 3.

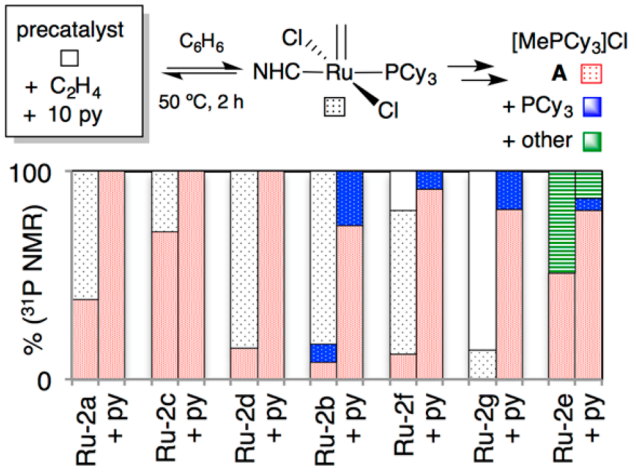

Figure 3. Accelerating effect of pyridine on decomposition of phosphine-stabilized catalysts under ethylene. Complexes grouped by behavior; for codes, see Chart 1.

For the benchmark H_2IMes catalyst **Ru-2a**, the dominant species present after 2 h at 50 °C in the absence of py was the resting-state methylidene complex **Ru-4a** (62% of total $^{31}P\{^1H\}$ NMR integration), the balance of material being due to **A**. In the presence of 10 py, formation of **A** was quantitative. Similar behavior was observed for the H_2IPr complex **Ru-2c** and IPr catalyst **Ru-2d**.

In the donor-free control experiments, the IPr and IMes systems (**Ru-2d** and **Ru-2b**, respectively) show a higher proportion of the methylidene species relative to their saturated analogues,[31] as expected given the stronger binding of phosphine ligands trans to an unsaturated NHC.[13] Importantly, however, the increased strength of the Ru−PCy_3 bond does not confer protection against donor-accelerated methylidene abstraction: like **Ru-2c**, the IPr complex **Ru-2d** undergoes complete decomposition to **A** within 2 h when ethylene and pyridine are simultaneously present, while the IMes derivative **Ru-2b** eliminates 74% **A**.[32] For the latter system, a minor contribution from an additional, unidentified pathway is implied by the observation of free PCy_3: 9% in the control

DOI: 10.1021/jacs.6b08372
J. Am. Chem. Soc. 2016, 138, 14668−14677

experiment, and 26% in the presence of pyridine. As noted above, ^{1}H NMR analysis shows no evidence of the pyridinium salt [MeNC$_5$H$_5$]Cl,[33] ruling out the possibility that pyridine competes for attack on the methylidene site.

The indenylidene catalysts **Ru-2f** and **Ru-2g** (bearing H$_2$IMes and IMes ligands, respectively) were far less active than the other systems examined. In the absence of pyridine, catalyst initiation was incomplete in both cases, with 19% **Ru-2f**, and 86% **Ru-2g**, remaining unreacted even after 2 h at 50 °C under ethylene. (As expected, the balance was chiefly the resting-state methylidene complexes **Ru-4a** or **Ru-4b**). Again, however, poor turnon efficiency does not protect against donor-accelerated methylidene abstraction. Both **Ru-2f** and **Ru-2g** showed >80% decomposition to **A** in the presence of pyridine (91% for **Ru-2f**; 82% for **Ru-2g**). We infer that pyridine binding accelerates initiation for these species, but that methylidene abstraction is competitive with metathesis. As with **Ru-2b**, a small proportion of free PCy$_3$ was also observed.

The H$_2$ITol derivative **Ru-2e** likewise exhibited >80% elimination of **A** following treatment with ethylene and pyridine. Also present was ca. 10% of an as-yet unidentified species, observed as a ^{31}P{^{1}H} NMR singlet at 48.1 ppm. No alkylidene signal was evident by ^{1}H NMR analysis, ruling out the possibility that this is simply a pyridine adduct of **Ru-2e** or its methylidene resting state. Complicating analysis is the presence of ca. 15% impurities in the commercial precatalyst (see Figure S15).[34] Identification of the unknown species was therefore not pursued.

In all cases, the [MePCy$_3$]Cl marker **A** was the dominant ^{31}P-containing species present after 2 h exposure to ethylene and pyridine at 50 °C. We conclude that abstraction of the methylidene ligand by phosphine is the major pathway operative, and that such abstraction is significantly accelerated by the Lewis donor pyridine.

Scope with Respect to Donor. Of keen interest is the extent to which Lewis bases other than pyridine and primary or secondary amines[19−21,35] accelerate methylidene abstraction. To examine this point, we treated **Ru-4a** and its less labile IMes analogue **Ru-4b** with a range of less potent donors at 50 °C. Shown in Table 1 is the proportion of **A** formed, vs **Ru-4** remaining, after 2 h. These figures should be compared to a baseline value of 10% or 3% for **Ru-4a** or **Ru-4b**, respectively, in the base-free control experiments (entry 1). Values for pyridine are shown as the final table entry, for comparison. In all cases, the trend seen with the IMes complex **Ru-4b** parallels that with **Ru-4a**. While stronger Ru−PCy$_3$ binding lessens the impact on decomposition rates, it also limits entry into the active cycle for metathesis.

The NEt$_3$, phosphoramide, and urea additives shown in entries 2−4 were chosen for the detrimental impact of these and related structures in other contexts, including in metathesis promoted by nonphosphine catalysts.[3,9,36−39] The absence of any significant impact for any of these indicates that the Lewis basicity of the donor is irrelevant, if steric congestion precludes access to the metal center.[40] This is consistent with the prior finding that added DBU did not trigger decomposition of **Ru-2a** into **A** during catalysis.[19]

Of note, even relatively weak donors such as MeCN, THF, and H$_2$O accelerate decomposition (entries 5−7). Addition of MeCN had minimal impact in small amounts (10 equiv), but decomposition was quantitative at 2 h in neat MeCN (entries 5a, 5b; see also Figure 4a). Similarly, while 10 equiv THF and H$_2$O proved relatively innocuous, a 10-fold increase led to ca. 30% or 50% decomposition, respectively, notwithstanding the weak oxophilicity of these ruthenium complexes. The heightened effect of water and methanol, relative to THF (entries 7a and 9, vs 6a), may be due to attractive hydrogen-bonding interactions with the chloride ligands. While additional decomposition pathways could be envisaged for these H-bond donors, **A** was the sole or dominant phosphorus product in all cases, indicating that methylidene abstraction is the principal vector for decomposition.

Accelerated methylidene abstraction by MeCN, THF, DMSO, H$_2$O, and MeOH helps to account for the suboptimal metathesis performance of phosphine-functionalized catalysts in these solvents.[41−45] More generally, it provides the first clear explanation for low metathesis productivities in polar media, despite the correlation between solvent polarity and faster initiation (phosphine loss) established for **Ru-2a**.[46] This behavior is of particular note given interest in metathesis in water and "green" solvents, often bearing ether donors.[43,44,47−49] The impact of water holds arguably even greater

Table 1. Loss of Ru-4 and Yield of [MePCy$_3$]Cl (A) on Treatment with L-Donors (n Equiv) for 2 h at 50 °C[a]

			% **Ru-4** lost (% **A** formed)	
entry	L-donor	n	(a) H$_2$IMes	(b) IMes
1	None	0	10 (10)	3 (N.D.)
2	NEt$_3$	10	11 (11)	3 (N.D.)
3	O=P(NMe$_2$)$_3$	10	13 (13)	3 (N.D.)
4	O=C(NMe$_2$)$_2$	10	16 (16)	3 (N.D.)
5a	MeCN	10	11 (11)	3 (N.D.)
5b		neat	100 (100)	–
6a	THF	10	20 (20)	8 (8)
6b		100	30 (30)	–
7a	H$_2$O	10	25 (25)	10 (10)
7b		100	49 (49)	–
8a	DMSO	10	35 (35)	18 (16)
8b		100	93 (93)	–
9	MeOH	10	49 (49)	29 (29)
10	pyridine	10	100 (100)[b]	100 (90)[c]

[a]C$_6$D$_6$ solvent, [Ru] = 20 mM. % Loss of **Ru-4** determined by ^{1}H NMR analysis, by integration of the methylidene signal vs internal standard (TMB); % **A** by ^{31}P{^{1}H} NMR analysis, as a percentage of total integration. N.D. = not determined; peak intensity insufficient for reliable ^{31}P NMR integration. **Ru-4** completes the mass balance, except where noted. [b]Complete in <10 min at RT. [c]For L = py, free PCy$_3$ accounts for the discrepancy between % **Ru-4b** lost and % **A** formed.

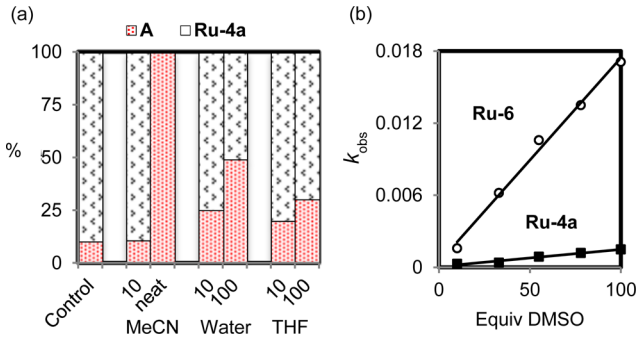

Figure 4. (a) Impact of donor stoichiometry on decomposition of RuCl$_2$(H$_2$IMes) (PCy$_3$)(=CH$_2$) **Ru-4a** (C$_6$D$_6$, 50 °C, 2 h; data from Table 1). (b) First-order dependence of decomposition rates on [DMSO] for **Ru-4a** and **Ru-6** at 25 °C. See Tables S3 and S4.

DOI: 10.1021/jacs.6b08372
J. Am. Chem. Soc. 2016, 138, 14668−14677

significance, given its ubiquity as a contaminant in synthetic and process chemistry.

Associative Mechanism and Implications. Rates of metathesis by **Ru-2a** and its analogues are independent of olefin concentration, because loss of PCy_3 is rate-limiting.[46] In the absence of donors, loss of PCy_3 likewise controls the rate of decomposition of the resting-state species **Ru-4a** and **Ru-4b**.[13,31] The rapidity with which these complexes decompose in the *presence* of donor ligands (see above) strongly suggests an associative pathway for the decomposition reaction, as does the impact of donor bulk and stoichiometry. For sterically accessible donors, coordination to the Ru center prior to PCy_3 loss would plausibly create a degree of steric pressure that promotes expulsion of the phosphine ligand.

To probe this point, **Ru-4a** was treated with varying concentrations of DMSO, with which decomposition is sufficiently slow to monitor at RT, and the rates of loss of **Ru-4a** (Figure 4b) and formation of **A** were measured. Both rates exhibit a first-order dependence on [DMSO]. Decomposition of the first-generation complex **Ru-6** was likewise first-order in [DMSO], but two notable differences emerged. First, the reaction was 5-fold faster (k_{obs} = 0.0003 and 0.0015 min^{-1} for **Ru-4a** and **Ru-6**, respectively). This is consistent with the reported[13] operation of the inverse trans effect in the NHC complex **Ru-4a**, which enhances the Ru−PCy_3 bond strength. Second, the rate of formation of **A** no longer corresponds to the rate of loss of **Ru-6**. This is consistent with displacement of both PCy_3 ligands from **Ru-6**, upon which the C−H activation step becomes rate-determining, as with the pyridine system shown in Scheme 2.[20]

While isolation of the σ-alkyl intermediate for the H_2IMes complex was precluded by facile C−H activation, as indicated above, the σ-alkyl complex $RuCl_2(\sigma\text{-}CH_2PCy_3)(DMSO)_3$ **Ru-9** decomposed slowly. Indeed, this complex could be isolated in ca. 60% yield following treatment of **Ru-6** with a 100-fold excess of DMSO (Scheme 3). Its molecular identity is

Scheme 3. σ-Alkyl Intermediates Accessible by Inhibiting C−H Activation of Ancillary Ligands

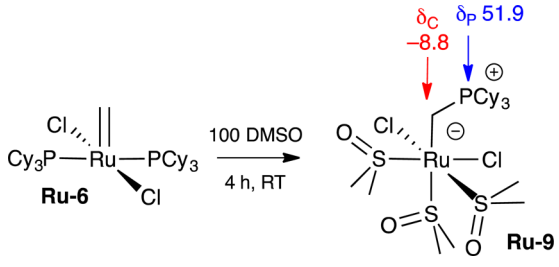

supported by NMR and combustion analysis. The fac,*S*-coordination mode is proposed on the basis of the predominance of this binding mode in other Ru−DMSO complexes.[50−52] IR evidence is consistent with *S*-binding (two strong ν(S=O) bands at 1072 and 1017 cm^{-1}, vs an expected value of ca. 950 cm^{-1} for the *O*-bound linkage isomer). The chemical shifts and multiplicities for the Ru−CH_2PCy_3 moiety agree well with those for pyridine analogue **Ru-7** (see Scheme 3 and Figure 2, left).[20] The stability of these species reflects the absence of a readily activated C−H bond, a consequence of the displacement of both PCy_3 ligands (see discussion above).

Rate-Determining Step. Within the H_2IMes system, the rapidity of the C−H activation step (k_4, Scheme 4) means that

Scheme 4. Shifting Rate-Limiting Step in Donor-Accelerated Methylidene Abstraction

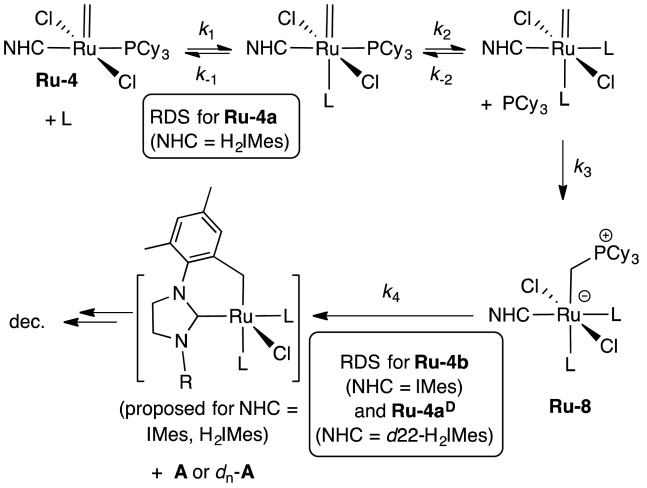

only the starting methylidene complex **Ru-4a** and decomposition product $[MePCy_3]Cl$ **A** are observed. Rate-determining L-binding is unsurprising, given steric constraints on approach of L to five-coordinate **Ru-4a** imposed by the cumulative bulk of the H_2IMes and PCy_3 ligands. Of note, however, the rate-determining step for the IMes system **Ru-4b** switches to C−H activation, as inferred from the fact that the σ-alkyl intermediate is observable. The energetic barriers to donor binding and to C−H activation are evidently very similar.

Corroboration of this point comes from deuterium-labeling studies using the d_{22}-H_2IMes complex **Ru-4a^D**, containing perdeuterated mesityl groups. On treating this labeled complex with pyridine, the σ-alkyl species **Ru-8a^D** could be observed at short reaction times (29% at 5 min, with essentially quantitative liberation of the phosphonium salts at 10 min). That is, deuteration is sufficient to change the rate-determining step from pyridine binding to C−H activation. A similar effect was evident with DMSO, with which decomposition was slower, and rate constants could be measured. The kinetic isotope effect (as judged from the k_H/k_D ratio), was 1.5,[53] at the low end for a primary kinetic isotope effect,[54] perhaps indicating that C−H activation is only partially rate-determining. An additional factor, however, may be competing H/D scrambling between the methylidene and the *o*-CD_3 groups (analogous to methylidene−cyclohexyl D−H exchange processes reported in the first-generation catalysts).[55] Thus, while ^{2}H NMR and MALDI-MS analysis of the products formed on decomposition of **Ru-4a^D** confirmed incorporation of a mesityl *o*-CD_3 deuteron as $[CH_2DPCy_3]Cl$, essentially equal amounts of nondeuterated **A** were also evident, accompanied by lesser proportions of the d_2-**A** and d_3-**A** isotopologues (22% and 8%, respectively; Figure S10).[56]

Consistent with intermolecular attack of free PCy_3 on the methylidene ligand, as shown in Schemes 1 and 4, decomposition of the IMes complex **Ru-4b** exhibits a rate dependence on [PCy_3] (as with **Ru-6**).[30] Thus, reaction with a 3-fold excess of pyridine under the conditions of Figure 1 resulted in complete decomposition within 50 min in the presence of 10 PCy_3, but required 75 min in the absence of added PCy_3 (Figure S14; Tables S2, S3).

In an important study of the first-generation benzylidene catalyst **Ru-1**, Diver, Keister and co-workers described related but distinct behavior on treatment with isocyanides.[17d]

DOI: 10.1021/jacs.6b08372
J. Am. Chem. Soc. 2016, 138, 14668−14677

Liberation of the ylide $PhCH{=}PCy_3$ **B** was observed, rather than the phosphonium salt $[(PhCH_2)PCy_3]Cl$ **A′** corresponding to **A**. Intramolecular 1,2-migration of the PCy_3 ligand onto the benzylidene carbon was proposed on the basis of a competition experiment involving addition of a 3-fold excess of P^nBu_3, in which the observed ratio of **B** to $PhCH{=}P^nBu_3$ (**B′**) was ca. 2:1, rather than the 1:3 ratio expected for the intermolecular pathway. The discrepancy may reflect steric differences between the benzylidene and methylidene complexes. Substitution at the Ru=CHR site may inhibit intermolecular approach of PR_3, instead favoring an intramolecular pathway. For the methylidene complexes, intermolecular attack of phosphine at the more accessible methylidene carbon ($[Ru]{=}CH_2$) is validated by our decomposition studies in the presence of added phosphine.

Impact on Metathesis. The drastically inhibiting impact of amines in metathesis reactions catalyzed by **Ru-2a** has been described elsewhere.[19] The rapidity of decomposition, and the coformation of **A**, testify to the capacity of such donors to accelerate methylidene abstraction. To assess the impact of weaker donors, we examined the metathesis productivities attainable for the readily cyclized diene diethyl diallylmalonate (**1**) in the presence of added water or methanol, or in neat THF, MeCN, or DMSO. The results are collected in Table 2.

Table 2. Donor-Accelerated Decomposition: Impact of Weak Donors on Metathesis Productivity[a]

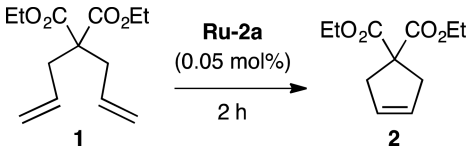

		% conv. (TON)[a]	
entry	solvent medium	50 °C	30 °C[58]
1	toluene	100 (2000)[b]	100 (2000)[c]
2	THF	72 (1440)	13 (260)
3	20:1 toluene–H_2O	35 (700)	24 (480)
4	20:1 toluene–MeOH	18 (360)	5 (100)
5	20:1 toluene–MeCN	13 (260)	17 (340)
6	20:1 toluene–DMSO	1 (20)	1 (20)

[a]Calibrated GC-FID analysis; ± 2% in replicate runs. [b]Quantitative within 10 min. [c]Quantitative within 60 min.

In the control experiment in anhydrous toluene, RCM was quantitative after 2 h at 50 °C at a catalyst loading of 0.05 mol %. This corresponds to a turnover number (TON) of 2,000. In neat THF, RCM activity dropped by more than 30%, to a TON of 1,440. The presence of 5% degassed H_2O in toluene caused a 65% drop in TON. With 5% MeOH, MeCN, and DMSO, the impact was even more detrimental: for the DMSO reaction, metathesis was essentially quenched. The ease with which **1** normally undergoes RCM underscores the severity of this degradation in metathesis performance.

Of note, reaction at 30 °C does not inhibit methylidene abstraction. Indeed, the impact of donors on total metathesis productivity was in general even more deleterious, in keeping with prior findings of faster increases in rates of metathesis as a function of temperature, relative to rates of decomposition.[9,57]

Of particular interest is the impact of the weak donor H_2O, which represents a ubiquitous contaminant in organic synthesis. To explicitly tie the presence of water to formation of **A** during catalysis, a related experiment was carried out with pro-lactone **3** (Scheme 5). Use of this substrate has the dual advantage of

Scheme 5. Evidence for Water-Accelerated Methylidene Abstraction During RCM Macrocyclization

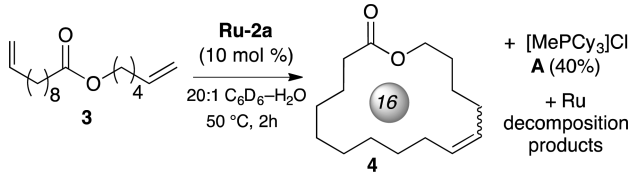

verifying the impact of water in an RCM reaction of broad interest, i.e., macrocyclization, while ensuring complete catalyst conscription at ruthenium loadings high enough to permit interrogation by NMR methods. Analysis after 2 h at 50 °C in 20:1 C_6D_6–H_2O indicated that **A** accounted for ca. 38% of the total $^{31}P\{^1H\}$ NMR integration, with ca. 50% being due to the resting-state methylidene complex **Ru-4a**. Also observed was a small amount of free PCy_3 (7%), and two minor, unidentified species (see SI, Figure S20). A control experiment confirmed that the proportion of **A** formed in the absence of water is substantially lower (7% **A**).

The Cazin group recently described the negative impact of water on RCM yields in the challenging cyclization of a derivative of diethyl diallylmalonate bearing geminally disubstituted olefins.[59] The present study is only the second report of the severely deleterious impact of water on Ru-catalyzed olefin metathesis: it is the first to demonstrate that even facile metathesis reactions are affected, and to advance a mechanistic basis for this behavior. While the present study does not rule out other, additional avenues for catalyst degradation, it clearly demonstrates that water significantly accelerates the methylidene-abstraction pathway.

Blocking Methylidene Abstraction. A final set of experiments examined the possibility that this decomposition pathway could be blocked by introducing a methyl substituent on the methylidene ligand. This question was inspired by reports of higher turnover numbers in metathesis when α-olefins were replaced by β-methyl olefins,[6,60−62] and by the trend in half-lives at 55 °C reported in the $RuCl_2(PCy_3)_2(=CHR)$ series: R = Ph, 8 days; R = Me, 8 h, R = H, 40 min.[55]

To test the resistance of the ethylidene moiety to abstraction by PCy_3, **Ru-10** was generated in situ in the presence of pyridine (Scheme 6). Complete conversion of **Ru-2a** into known[15] **Ru-10** and bis-pyridine adduct **Ru-11** (70:30) was

Scheme 6. Resistance of Ethylidene Ligand to Nucleophilic Abstraction by PCy_3

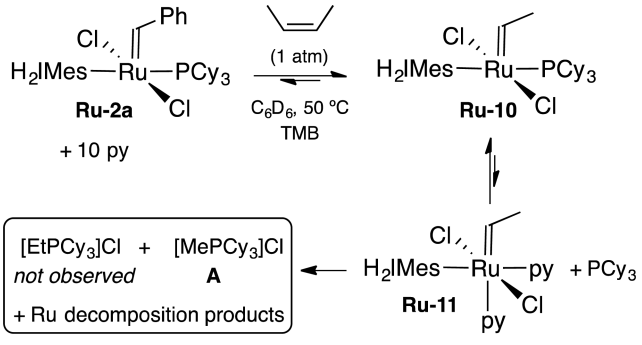

DOI: 10.1021/jacs.6b08372
J. Am. Chem. Soc. 2016, 138, 14668−14677

evident after 1 h at 50 °C. Decomposition occurred over ca. 48 h, as compared to the time scale of minutes at RT for the methylidene complex **Ru-4a**. Unexpectedly, NMR analysis revealed that the major ^{31}P-containing product was [$MePCy_3$]Cl **A** (34.2 ppm; 56% of total integration)—despite the evidence for complete formation of the ethylidene complex—accompanied by PCy_3 (10.5 ppm, 34%) and an unidentified product (47.2 ppm, 10%). The identity of **A** was confirmed by MALDI-TOF mass spectrometry; no signal was observed for [$EtPCy_3$]Cl. We attribute liberation of **A** to isomerization of 2-butene into 1-butene (observed by ^{1}H NMR analysis), metathesis of which enables partial formation and decomposition of **Ru-4a**. These results indicate that use of 2-butene in cross-metathesis is an incomplete solution to the problem of catalyst decomposition. More fundamentally, they demonstrate that the ethylidene moiety indeed resists donor-accelerated decomposition, offering the first clear insight into the superior metathesis performance attainable with β-methyl olefins, vs α-olefins.

CONCLUSIONS

The foregoing demonstrates that the resting-state methylidene complexes formed by phosphine-stabilized metathesis catalysts are subject to a common decomposition pathway: specifically, abstraction of the methylidene ligand as [$MePCy_3$]Cl **A**. Sterically accessible Lewis donors are shown to accelerate this process, at rates that depend on donor concentration. Because of the associative nature of this pathway, even rather feeble donors such as THF, H_2O, and MeOH are able to promote decomposition when present in significant amounts, with drastic consequences even for metathesis of readily cyclized substrates such as diethyl diallylmalonate. These results highlight the limited compatibility of phosphine-functionalized metathesis catalysts with substrates bearing a terminal olefin. Wherever sterically accessible donor functionalities are present (whether in the solvent, within the substrate structure, or in contaminants), they can trigger irreversible loss of the critical methylidene moiety from the active species. Installation of a β-methyl substituent is shown to circumvent this catalyst decomposition pathway.

EXPERIMENTAL SECTION

General Procedures. Reactions were carried out in an N_2-filled glovebox at room temperature (25 ± 2 °C), unless otherwise indicated. Solvents were purified as described below, then stored under N_2 in the glovebox over 4 Å molecular sieves (except MeOH: stored over 3 Å sieves) for at least 16 h prior to use. HPLC-grade C_6H_6, C_7H_8 and THF (Fisher) were dried and degassed using a Glass Contour solvent purification system (water content prior to sieve treatment, as measured by Karl Fischer titration: C_6H_6, 4 ppm; C_7H_8, 4 ppm; THF, 10 ppm). MeOH was distilled from magnesium turnings, pentane from P_2O_5 after predrying over $MgSO_4$, DMSO (>99%, BDH), MeCN (>99%, Fisher), pyridine (>99%, Fisher) and NEt_3 (99%, Alfa Aesar) from CaH_2. Deionized H_2O was degassed by five consecutive freeze/pump/thaw cycles, as was C_6D_6 (Cambridge Isotopes). CD_2Cl_2 (Cambridge Isotopes) was purchased in sealed ampules and used as received. Hexamethylphosphoramide, tetramethylurea (both 99%, Sigma-Aldrich), dodecane (>99%, Sigma-Aldrich) and diethyl diallylmalonate (**1**; 98%, Sigma-Aldrich) were freeze−thaw degassed as above. Ruthenium catalysts **Ru-2c**, **Ru-2e** (Sigma-Aldrich), **Ru-2f** and **Ru-2g** (Strem) were used as received, as were potassium hydrotris(1-pyrazolyl)borate KTp (>99%, Sigma-Aldrich), trimethoxybenzene (TMB, Sigma-Aldrich), ethylene (BOC Ultra-High Purity grade 3.0, 99.9%; Linde), ^{13}C-labeled ethylene (99% ^{13}C-enriched; Sigma-Aldrich), and *cis*-2-butene (>99%, GFS Chemicals). 1-Methylpyridinium chloride [$MeNC_5H_5$]Cl (>98%, TCI Chemicals) was dried under vacuum at 30 °C for 24 h prior to NMR analysis. Literature procedures were used to prepare the following: IMes,[63] **Ru-2a**,[64] **Ru-2b**,[64] **Ru-2d**,[65] **Ru-6**,[66] **Ru-4a**,[66] ***Ru-4a**,[21] **Ru-4b**[66] (the reported[21] improved workup was used for **Ru-4a** and **Ru-4b**), d_{22}-H_2IMes·HCl[22d] and pro-lactone **3**.[67] NMR spectra were recorded at 23 ± 2 °C, and referenced against the residual proton or carbon signals of the deuterated solvents (^{1}H, ^{13}C) or 85% H_3PO_4 (^{31}P). Elemental analysis was carried out by MHW Laboratories (Phoenix, AZ). GC quantification was performed on samples diluted with CH_2Cl_2 (ACS reagent grade) on an Agilent 7890A Series autosampler and an Agilent HP-5 polysiloxane column (30 m length, 320 μm diameter), using an inlet split ratio of 10:1, an inlet temperature of 250 °C, and helium (UHP grade) as the carrier gas to maintain column pressure at 11.512 psi. The FID response was maintained between 50 and 2000 ρA, using analyte concentrations of ca. 5 mM. Calibration curves (peak areas vs concentration) were constructed in the relevant concentration regime for substrates **1** and **3**, and their RCM products **2** and **4**. Conversions and yields in catalytic runs were determined from the integrated peak areas, relative to dodecane as internal standard, and compared to the initial integration ratio of substrate to dodecane. IR data were collected on a Nicolet 6700 FT-ATR IR spectrometer. Mass spectra were recorded on a Bruker Daltonics UltraFleXtreme MALDI time-of-flight mass spectrometer interfaced to a glovebox.

Synthesis of $RuCl_2$(IMes)(PCy_3)(=$^{13}CH_2$), *Ru-4b. Prepared as described for ***Ru-4a**,[21] using IMes in place of H_2IMes. Yield of ***Ru-4b**: 102 mg (50%; 99.5% ^{13}C-enriched). Isolated yields are adversely affected by partial solubility in the solvents used to extract PCy_3 and ***A**. Chemical shifts are in excellent agreement with the values reported for the nonlabeled isotopologue, with added ^{13}C coupling. ^{31}P{^{1}H} (121 MHz, C_6D_6): δ 40.9 (d, $^2J_{PC}$ = 9.5 Hz). ^{1}H NMR (300 MHz, C_6D_6): δ 18.76 (d, $^1J_{HC}$ = 157.8 Hz, 2H, Ru=CH_2), 6.90 (s, 2H, Mes *m*-C*H*), 6.72 (s, 2H, Mes *m*-C*H*), 6.23 (br s, 1H, NC*H*=), 6.13 (br s, 1H, NC*H*=), 2.60 (s, 6H, *o*-CH_3), 2.47−2.27 (overlapping, 9H, *o*-CH_3 and Cy), 2.19 (s, 3H, *p*-CH_3), 2.11 (s, 3H, *p*-CH_3), 1.78−1.47 (m, 15H, Cy), 1.29−1.01 (m, 15H, Cy). ^{13}C{^{1}H} (75 MHz, C_6D_6) (methylidene signal only): δ 295.4 (d, $^2J_{CP}$ = 9.5 Hz, Ru=CH_2). For spectra, see Figure S2.

Synthesis of $RuCl_2$(d_{22}-H_2IMes)(PCy_3)(=CH_2) Ru-4a^D. The deuterium-labeled compound was prepared according to the method established for nonlabeled **Ru-4a**,[66] but using free d_{22}-H_2IMes. The free carbene was generated[68] and installed by the reported methods.[66] NMR chemical shifts agree with with the values reported for the nonlabeled species.

Decomposition of Grubbs Methylidene Complexes by Pyridine. In a representative procedure, a screw-cap NMR tube was charged with **Ru-4b** (230 μL of a 43 mM stock solution in C_6D_6; 0.012 mmol), TMB (ca. 1 mg), and C_6D_6 (350 μL), to obtain a final Ru concentration of 20 mM. A ^{1}H NMR spectrum was recorded to establish the initial integration ratio of **Ru-4b** vs TMB. Pyridine (24 μL of a 1.3 M stock solution in C_6D_6; 3 equiv) was injected at the NMR instrument. An immediate color change from yellow-brown to deep red resulted, with turbidity developing within minutes. The septum was covered with Parafilm, the tube shaken well, and ^{31}P NMR acquisition was immediately initiated. Spectra were collected at 5 min intervals for the first 50 min, then at 75 min (see SI). A transient signal assigned to **Ru-8b** (see below) was observed over the period 3−45 min. Complete loss of starting **Ru-4b** was evident at 75 min. ^{31}P{^{1}H} NMR values are reported as a percentage of total integration ^{31}P{^{1}H} (121 MHz, C_6D_6): δ 34.2 (s, [$MePCy_3$]Cl **A**, 89%), 10.4 (s, PCy_3, 11%). See Figure 1, Figure S7 and Table S2. With 10 equiv py, at 10 min, full decomposition is seen: ^{31}P{^{1}H} (121 MHz, C_6D_6): δ 34.2 (s, **A**, 81%), 10.4 (s, PCy_3, 19%).

Impact of [PCy_3] on Rate of Decomposition of Ru-4b by Pyridine. As above but with 10 equiv PCy_3 added. Complete loss of starting **Ru-4b** was evident at 50 min. ^{31}P{^{1}H} (121 MHz, C_6D_6): δ 34.2 (s, [$MePCy_3$]Cl **A**, 91%), 10.4 (s, PCy_3, 9%). See Figure S14b and Table S3.

Decomposition of IMes Derivative *Ru-4b by Pyridine: Direct Observation of σ-Alkyl Intermediate

DOI: 10.1021/jacs.6b08372
J. Am. Chem. Soc. 2016, 138, 14668−14677

$RuCl_2(\sigma\text{-}^{13}CH_2PCy_3)(IMes)(py)_2$, *Ru-8b. Procedure as indicated for **Ru-4b** and pyridine. $^{13}C\{^1H\}$ (75 MHz, C_6D_6; collected over 2−16 min, 512 scans, key signals only): δ 295.4 (d, $^2J_{CP}$ = 9.5 Hz, Ru=CH_2, ***Ru-4b**), 1.2 (d, $^1J_{PC}$ = 47.8 Hz, [$^{13}CH_3PCy_3$]Cl) ***A**, −27.4 (d, $^1J_{PC}$ = 11.6 Hz, Ru-CH_2PCy_3). $^{31}P\{^1H\}$ (121 MHz, C_6D_6; collected over 16−22 min, 200 scans): δ 61.3 (d, $^1J_{PC}$ = 11.6 Hz, ***Ru-8b**, 6%), 40.9 (d, $^2J_{PC}$ = 9.5 Hz, ***Ru-4b**, 32%), 34.2 (d, $^1J_{PC}$ = 47.8 Hz, [$^{13}CH_3PCy_3$]Cl ***A**, 54%), 10.4 (s, free PCy_3, 8%). See Figure S8. At 75 min: $^{31}P\{^1H\}$ (121 MHz, C_6D_6): δ 34.2 (d, $^1J_{PC}$ = 47.8 Hz, [$^{13}CH_3PCy_3$]Cl ***A**, 90%), 10.4 (s, PCy_3, 10%); no Ru-phosphine species apparent.

Decomposition of $RuCl_2(H_2IMes)(PCy_3)(=^{13}CH_2)$ *Ru-4a by Pyridine. As for **Ru-4b** above, using 10 equiv pyridine. No signal for **Ru-4a** was apparent after 5 min. $^{31}P\{^1H\}$ (121 MHz, C_6D_6): δ 34.2 (d, $^1J_{PC}$ = 47.8 Hz, [$^{13}CH_3PCy_3$]Cl ***A**, 87%), 10.4 (s, PCy_3, 13%).

Decomposition of $RuCl_2(d_{22}\text{-}H_2IMes)(PCy_3)(=CH_2)$ Ru-4a^D by Pyridine. As for ***Ru-4a** above. Analysis at 5 min: $^{31}P\{^1H\}$ (121 MHz, C_6D_6): δ 60.1 (s, **Ru-8a^D**, 29%), 34.09−34.17 (m, d_n-**A**, 57%), 10.4 (s, PCy_3, 14%). At 10 min (full decomposition): $^{31}P\{^1H\}$ (121 MHz, C_6D_6): δ 34.2 (m, d_n-**A**, 87%), 10.5 (s, PCy_3, 13%). MALDI-TOF MS (pyrene matrix;[69] *m*/*z*): 295.256 ($C_{19}H_{36}P$, **A**; calcd 295.255), 296.261 ($C_{19}H_{35}DP$, d_1-**A**, calcd 296.262), 297.267 ($C_{19}H_{34}D_2P$, d_2-**A**; calcd 297.268); 298.277 ($C_{19}H_{33}D_3P$, d_3-**A**; calcd 298.274). See Figures S9, S10.

Decomposition of In Situ-Generated Methylidene Complexes by Pyridine. In a representative procedure, a 25 mL Schlenk tube equipped with a Kontes tap was loaded with **Ru-2b** (10 mg, 0.01 mmol) and 2 mL C_6H_6. The solution was freeze−pump−thaw degassed three times, and allowed to thaw under ethylene. Pyridine (8 μL, 0.1 mmol, 10 equiv) was added via syringe against a positive pressure of ethylene. The flask was sealed, returned to the glovebox, and heated at 50 °C. A color change from pink to orange-red occurred within minutes. After 2 h, a C_6D_6 spike was added, and the $^{31}P\{^1H\}$ NMR spectrum was measured. $^{31}P\{^1H\}$ (121 MHz, C_6D_6): δ 34.2 (s, [$MePCy_3$]Cl **A**, 74%), 10.5 (s, PCy_3, 26%. See Figure S11b (for the control experiment with **Ru-2b** under ethylene in the absence of pyridine, see Figure S11a). Table S1 summarizes the data for all catalysts studied.

Representative Procedure for Reaction of Ru-4a or Ru-4b with Lewis Donors. Experiments carried out as above, with the following modifications. The donor was added in the glovebox following measurement of the initial ratio of **Ru-4a** to TMB; the sample was shaken well and transferred to an oil bath set at 50 °C for 2 h. For DMSO (10 equiv): $^{31}P\{^1H\}$ NMR (121 MHz, C_6D_6): δ 38.2 (s, **Ru-4a**, 65%), 34.2 (s, [$MePCy_3$]Cl **A**, 35%). ^1H NMR (300 MHz, C_6D_6): δ 18.42 (s, **Ru-4a**, 65%). For control experiment without donor, see Figure S12; for representative spectra for the DMSO experiment above, see Figure S13.

Variants. For H_2O and THF, corresponding experiments were carried out with 100 equiv R_2O; for MeCN, with neat MeCN; see Figure 4a in main text. Kinetics studies were carried out with 10, 33, 55, 78, and 100 equiv DMSO at RT and monitored for 27 h: see Figure 4b, Table S4 (data) and Table S5 (half-lives and rate constants).

Synthesis of $RuCl_2(\sigma\text{-}CH_2PCy_3)(DMSO)_3$, Ru-9. To a stirred solution of **Ru-6** (131 mg, 0.175 mmol) in C_6H_6 (8 mL) in a 25 mL Schlenk flask was added DMSO (1.24 mL 1.37 g, 17.5 mmol, 100 equiv). A color change from pink to yellow occurred over 2 h, but reaction was incomplete (95% conversion). After 4 h, no further **Ru-6** was present by ^{31}P NMR analysis. Pentane (20 mL) was added to precipitate pale yellow **Ru-9**, which was filtered off and washed with cold pentane (5 × 2 mL). Yield 74 mg (60%, 0.11 mmol). $^{31}P\{^1H\}$ NMR (121.5 MHz, C_6D_6): δ 51.9 (s). ^1H NMR (300 MHz, C_6D_6): δ 3.34 (overlapping s, 12H, $((CH_3)_2SO)_2$, 3.19 (s, 6H, $((CH_3)_2SO)$), 3.06−2.95 (m, 3H, Cy), 2.25−2.15 (m, 6H, Cy), 1.71−1.55 (m, 10H, Cy), 1.42−1.27 (m, 12H, Cy), 1.13−1.04 (m, 2H, Cy), 0.96 (d, 2H, $^2J_{HP}$ = 15.2 Hz, Ru−CH_2PCy_3). $^{13}C\{^1H\}$ (75 MHz, C_6D_6; selected): δ −8.8 (d, $^1J_{PC}$ = 22.2 Hz, Ru-CH_2PCy_3). Experiments supporting assignment of the σ−CH_2PCy_3 doublet at 0.96 ppm: ^1H−^{13}C HMQC correlation with $^{13}C\{^1H\}$ NMR doublet at −8.8 ppm; ^1H−^{31}P HMQC correlation with $^{31}P\{^1H\}$ NMR singlet at 51.9 ppm; ^1H−^1H COSY, no correlation. ATR-IR: ν(S=O) 1072, 1017 cm^{-1} (s, *S*-bonded DMSO). Anal. Calc'd. for $C_{25}H_{53}Cl_2O_3PRuS_3$: C, 42.85; H, 7.62. Found: C, 43.05; H, 7.75. For spectra, see Figures S3−S6.

Impact of Donors on RCM. A Schlenk tube was loaded with diethyldiallyl malonate **1** (48 mg, 0.2 mmol), dodecane (34 mg, 0.2 mmol; internal standard), H_2O (90 μL, 0.01 mmol) and toluene (1.8 mL). An aliquot was removed for GC-FID analysis to establish the starting ratio of **DDM** to dodecane. To the flask was added catalyst **Ru-2a** from a stock solution in toluene (33 μL of a 3.0 mM solution containing 12.8 mg **Ru-2a** in 5.0 mL toluene; 0.001 mmol, 0.05 mol %). The reaction was heated for 2 h at 50 ± 1 °C in an oil bath in the glovebox. A sample was then removed, quenched with KTp (10 mg/mL in THF; 10 equiv vs **Ru-2a**), and analyzed by GC-FID; see Figure S17.

Evidence for Water-Accelerated Methylidene Abstraction During RCM Macrocyclization. In the glovebox, a J. Young NMR tube was charged with **Ru-2a** (11.6 mg, 0.0137 mmol), prolactone **3** (33.7 mg, 0.137 mmol, 10 equiv), 0.67 mL C_6D_6, and degassed H_2O (35 μL, 20:1 v/v vs C_6D_6 solvent). The sample was heated at 50 °C as for DDM. A color change from pink to orange occurred within the first 20 min. Phosphorus speciation at 2 h: $^{31}P\{^1H\}$ NMR (121 MHz, C_6D_6; as % of total integration): δ 38.2 (s, **Ru-4a**, 50%), 33.9 (s, [$MePCy_3$]Cl **A**, 38%), 31.1 (3%, unassigned), 29.1 (3%, unassigned), free PCy_3 (10.4 ppm, 6%). See Figure S20. No **Ru-2a** (30.1 ppm) remained. The signal for **A** is broadened ($\omega_{1/2}$ 33 Hz) and its chemical shift ca. 0.3 ppm upfield relative to the values above, perhaps indicating H-bonding with water.

Reaction of $RuCl_2(H_2IMes)(PCy_3)(=CHMe)$ Ru-10 (Generated In Situ) with Pyridine. A solution of **Ru-2a** (10 mg, 0.012 mmol), 600 μL C_6D_6, and TMB (ca. 1 mg; internal standard) was prepared and analyzed (^1H NMR) to establish the initial integration ratio of **Ru-2a** vs TMB. Pyridine (10 μL, 0.12 mmol, 10 equiv) was added, and the solution was freeze−pump−thaw degassed (3×) and allowed to thaw under an atmosphere of *cis*-2-butene. The NMR tube was then sealed and heated at 50 °C in a thermostated oil-bath in the glovebox. Decomposition rates were established by NMR analysis. Key signals at 1 h (see Figure S18): ^1H NMR (300 MHz, C_6D_6) δ 19.67 (q, $^3J_{HH}$ = 6.4 Hz, $RuCl_2(H_2IMes)(py)_2(=CHMe)$ **Ru-11**, 30%), 18.99 (q of d, $^3J_{HH}$ = 5.5 Hz, $^2J_{HP}$ = 0.7 Hz, **Ru-10**, 70%). $^{31}P\{^1H\}$ NMR (121.5 MHz, C_6D_6): δ 28.99 (s, **Ru-10**, 70%), 10.5 (s, free PCy_3, 30%). At 48 h (Figure S19): $^{31}P\{^1H\}$ NMR (121.5 MHz, C_6D_6) δ 47.2 (s, unidentified, 11%), 34.2 (s, [$MePCy_3$]Cl **A**, 56%), 10.5 (s, free PCy_3, 35%). MALDI-TOF MS (*m*/*z*): 295.26, [$MePCy_3$]Cl **A** (Calcd *m*/*z* for $[C_{19}H_{36}P]^+$: 295.26). No signal observed for [$EtPCy_3$]Cl (Calc'd *m*/*z* for $[C_{20}H_{38}P]^+$: 309.27).

Control Experiment: Decomposition of In Situ-Generated $RuCl_2(H_2IMes)(PCy_3)(=CHMe)$ Ru-10 in the Absence of Pyridine. Complete decomposition was evident after 15 days. Key signals at 1 h: ^1H NMR (300 MHz, C_6D_6) δ 18.99 (q of d, $^3J_{HH}$ = 5.5 Hz, $^2J_{HP}$ = 0.7 Hz, **Ru-10**, 100%). $^{31}P\{^1H\}$ NMR (121.5 MHz, C_6D_6): δ 28.99 (s, **Ru-10**, 100%). After 15 days: $^{31}P\{^1H\}$ NMR (121.5 MHz, C_6D_6) δ 71.8 (s, unidentified, 5%), 71.2 (s, unidentified, 7%), 47.2 (s, unidentified, 12%), 34.2 (s, [$MePCy_3$]Cl **A**, 75%).

■ ASSOCIATED CONTENT

Ⓢ Supporting Information

The Supporting Information is available free of charge on the ACS Publications website at DOI: 10.1021/jacs.6b08372.

NHC structures; NMR spectra for new complexes, impure H_2ITol complex **Ru-2e** and decomposition experiments; tabulated data for kinetics studies; ^2H NMR and MALDI-TOF MS evidence for the deuterated phosphonium salts, and a representative GC trace from catalysis (PDF)

■ AUTHOR INFORMATION

Corresponding Author

*dfogg@uottawa.ca

DOI: 10.1021/jacs.6b08372
J. Am. Chem. Soc. 2016, 138, 14668−14677

Notes

The authors declare no competing financial interest.

■ ACKNOWLEDGMENTS

NSERC is thanked for financial support, and Dr. Emma Davy (Fogg group) for Karl Fischer measurements of water content in organic solvents. Valuable discussions with Dr. Carolyn Higman, Prof. Jeffrey Keillor and Prof. Steve Diver are gratefully acknowledged.

■ REFERENCES

(1) Grela, K. *Olefin Metathesis—Theory and Practice*; Wiley: Hoboken, NJ, 2014.
(2) Grubbs, R. H.; Wenzel, A. G. *Handbook of Metathesis*, 2nd ed.; Wiley-VCH: Weinheim, 2015.
(3) Higman, C. S.; Lummiss, J. A. M.; Fogg, D. E. *Angew. Chem., Int. Ed.* **2016**, *55*, 3552−3565.
(4) Farina, V.; Horváth, A. Ring-Closing Metathesis in the Large-Scale Synthesis of Pharmaceuticals. In *Handbook of Metathesis*; Grubbs, R. H., Wenzel, A. G., Eds.; Wiley-VCH: Weinheim, 2015; Vol. 2, pp 633−658.
(5) Fandrick, K. R.; Savoie, J.; Jinhua, N. Y.; Song, J. J.; Senanayake, C. H. Challenges and Opportunities for Scaling the Ring-Closing Metathesis Reaction in the Pharmaceutical Industry. In *Olefin Metathesis—Theory and Practice*; Grela, K., Ed.; Wiley: Hoboken, 2014; pp 349−366.
(6) Pederson, R. L.; Nickel, A. Commercial Potential of Olefin Metathesis of Renewable Feedstocks. In *Olefin Metathesis—Theory and Practice*; Grela, K., Ed.; Wiley: Hoboken, NJ, 2014; pp 335−348.
(7) Chadwick, J. C.; Duchateau, R.; Freixa, Z.; van Leeuwen, P. W. N. M. *Homogeneous Catalysts: Activity−Stability−Deactivation*; Wiley-VCH: Weinheim, 2011.
(8) Hubner, S.; de Vries, J. G.; Farina, V. *Adv. Synth. Catal.* **2016**, *358*, 3−25.
(9) van Lierop, B. J.; Lummiss, J. A. M.; Fogg, D. E. Ring-Closing Metathesis. In *Olefin Metathesis—Theory and Practice*; Grela, K., Ed.; Wiley: Hoboken, NJ, 2014; pp 85−152.
(10) For the poor kinetic competence of molecular hydride species often cited as potential culprits, see: (a) Higman, C. S.; Plais, L.; Fogg, D. E. *ChemCatChem* **2013**, *5*, 3548−3551. For the involvement of Ru nanoparticles formed following loss of $[MePCy_3]Cl$ from **Ru-2a**, see: (b) Higman, C. S.; Lanterna, A. E.; Marin, M. L.; Scaiano, J. C.; Fogg, D. E. *ChemCatChem* **2016**, *8*, 2446−2449.
(11) Hughes, D. L. *Org. Process Res. Dev.* **2016**, *20*, 1008−1015.
(12) Styrenyl ether-stabilized catalysts of the Hoveyda class, in contrast, readily enter the active cycle for metathesis, as indicated by experiments with a ^{13}C-labelled styrenyl ether. See: Bates, J. M.; Lummiss, J. A. M.; Bailey, G. A.; Fogg, D. E. *ACS Catal.* **2014**, *4*, 2387−2394.
(13) Lummiss, J. A. M.; Higman, C. S.; Fyson, D. L.; McDonald, R.; Fogg, D. E. *Chem. Sci.* **2015**, *6*, 6739−6746.
(14) Lummiss, J. A. M.; Perras, F. A.; Bryce, D. L.; Fogg, D. E. *Organometallics* **2016**, *35*, 691−698.
(15) Sponsler and co-workers pointed out the corresponding labilizing effect of alkylidene substituents on metathesis reactivity. See: Williams, J. E.; Harner, M. J.; Sponsler, M. B. *Organometallics* **2005**, *24*, 2013−2015.
(16) Hong, S. H.; Wenzel, A. G.; Salguero, T. T.; Day, M. W.; Grubbs, R. H. *J. Am. Chem. Soc.* **2007**, *129*, 7961−7968.
(17) For precedents for attack of phosphine on a [Ru]=CHR carbon in complexes related to **Ru-2a**, see: (a) Burrell, A. K.; Clark, G. R.; Rickard, C. E. F.; Roper, W. R.; Wright, A. H. *J. Chem. Soc., Dalton Trans.* **1991**, 609−614. (b) Werner, H.; Stuer, W.; Weberndorfer, B.; Wolf, J. *Eur. J. Inorg. Chem.* **1999**, *1999*, 1707−1713. (c) Hansen, S. M.; Rominger, F.; Metz, M.; Hofmann, P. *Chem. - Eur. J.* **1999**, *5*, 557−566. (d) Galan, B. R.; Pitak, M.; Keister, J. B.; Diver, S. T. *Organometallics* **2008**, *27*, 3630−3632. See below for evidence supporting the intermolecular pathway depicted in Scheme 1.
(18) Methylidene abstraction was reportedly slow for **Ru-4a** at 55 °C, requiring 3 days for complete decomposition. See: ref 16. In separate experiments, we measured a decomposition half-life of ca. 160 min at 60 °C (specifically, 53% loss of alkylidene signals, 45% **A** (ref 14)), a figure in good agreement with the value of 144 min measured in ref 19.
(19) Lummiss, J. A. M.; Ireland, B. J.; Sommers, J. M.; Fogg, D. E. *ChemCatChem* **2014**, *6*, 459−463.
(20) Lummiss, J. A. M.; McClennan, W. L.; McDonald, R.; Fogg, D. E. *Organometallics* **2014**, *33*, 6738−6741.
(21) Lummiss, J. A. M.; Botti, A. G. G.; Fogg, D. E. *Catal. Sci. Technol.* **2014**, *4*, 4210−4218.
(22) For selected examples of the C−H activation of mesityl *o*-methyl groups in ruthenium complexes of H_2IMes and IMes, see ref 16 and: (a) Jazzar, R. F. R.; Macgregor, S. A.; Mahon, M. F.; Richards, S. P.; Whittlesey, M. K. *J. Am. Chem. Soc.* **2002**, *124*, 4944−4945. (b) Chilvers, M. J.; Jazzar, R. F. R.; Mahon, M. F.; Whittlesey, M. K. *Adv. Synth. Catal.* **2003**, *345*, 1111−1114. (c) Abdur-Rashid, K.; Fedorkiw, T.; Lough, A. J.; Morris, R. H. *Organometallics* **2004**, *23*, 86−94. (d) Leitao, E. M.; Dubberley, S. R.; Piers, W. E.; Wu, Q.; McDonald, R. *Chem. - Eur. J.* **2008**, *14*, 11565−11572. (e) Endo, K.; Herbert, M. B.; Grubbs, R. H. *Organometallics* **2013**, *32*, 5128−5135.
(23) For leading references, see ref 13 and: (a) Comas-Vives, A.; Harvey, J. N. *Eur. J. Inorg. Chem.* **2011**, *2011*, 5025−5035. (b) Vummaleti, S. V. C.; Nelson, D. J.; Poater, A.; Gomez-Suarez, A.; Cordes, D. B.; Slawin, A. M. Z.; Nolan, S. P.; Cavallo, L. *Chem. Sci.* **2015**, *8*, 1895−1904.
(24) Fernandez, I.; Lugan, N. l.; Lavigne, G. *Organometallics* **2012**, *31*, 1155−1160.
(25) Credendino, R.; Falivene, L.; Cavallo, L. *J. Am. Chem. Soc.* **2012**, *134*, 8127−8135.
(26) Gallagher, M. M.; Rooney, A. D.; Rooney, J. J. *J. Organomet. Chem.* **2008**, *693*, 1252−1260.
(27) Kotyk, M. W.; Gorelsky, S. I.; Conrad, J. C.; Carra, C.; Fogg, D. E. *Organometallics* **2009**, *28*, 5424−5431.
(28) Sanford, M. S.; Love, J. A.; Grubbs, R. H. *Organometallics* **2001**, *20*, 5314−5318.
(29) Conrad, J. C.; Yap, G. P. A.; Fogg, D. E. *Organometallics* **2003**, *22*, 1986−1988.
(30) Independent decomposition experiments with first-generation complex **Ru-6** support an intermolecular pathway, even in the absence of added donors. Thus, a half-life of 67 ± 3 h was measured for **Ru-6** at 22 °C in C_6D_6, but this figure dropped to 13.5 ± 0.2 h when 10 equiv PCy_3 was present. The stability of this complex exhibits a nonlinear dependence on temperature.
(31) The background reaction, i.e., methylidene abstraction in the absence of an added donor, was shown to be dissociative in PCy_3 in experiments carried out on the **Ru-4a** system. See: refs 13 and 16. For a detailed kinetics derivation, see Supporting Information for ref 13.
(32) A slight increase in the proportion of PCy_3 was observed under ethylene, relative to the experiments with the isolated methylidene complexes **Ru-4b**. This is consistent with the operation of additional elimination pathways in the presence of ethylene. See: van Rensburg, W. J.; Steynberg, P. J.; Meyer, W. H.; Kirk, M. M.; Forman, G. S. *J. Am. Chem. Soc.* **2004**, *126*, 14332−14333.
(33) The poor solubility of the pyridinium salt in nonpolar solvents (confirmed with an authentic sample of $[MeNC_6H_5]Cl$) could mask its presence in this experiment. The benzene solvent was therefore evaporated, and the residue redissolved in $CDCl_3$. The ^1H NMR spectrum showed no evidence of the diagnostic methyl singlet seen for authentic samples at 4.79 ppm in $CDCl_3$ (see Figure S16).
(34) These impurities may also contribute to elimination of A from the resting-state complex **Ru-4e**. However, the commercial availability of the precatalyst **Ru-2e** has been discontinued owing to problems with decomposition on long-term storage. It has been replaced by its phosphine-free styrenyl ether analogue. Personal Communication, John Phillips, Catalyst R&D, Materia, Inc.
(35) Half-lives for decomposition of $RuCl_2(H_2IMes)(PCy_3)(=CH_2)$ **Ru-4a** on addition of 1 equiv L (20 mM Ru, C_6D_6). At RT: with H_2N^nBu, <3 min; with pyrrolidine, 87 min; with morpholine, 14 h;

DOI: 10.1021/jacs.6b08372
J. Am. Chem. Soc. 2016, 138, 14668−14677

with DBU, >24 h, as compared to >24 h in the absence of added L. At 60 °C: with H_2N^nBu, <3 min; with pyrrolidine, 8 min; with morpholine, 35 min; with DBU, 127 min (ref 19); cf. 144 min in the absence of added L (see: ref 18).
(36) Wang, H.; Matsuhashi, H.; Doan, B. D.; Goodman, S. N.; Ouyang, X.; Clark, W. M. *Tetrahedron* **2009**, *65*, 6291−6303.
(37) Wang, H.; Goodman, S. N.; Dai, Q.; Stockdale, G. W.; Clark, W. M. *Org. Process Res. Dev.* **2008**, *12*, 226−234.
(38) Ireland, B. J.; Dobigny, B. T.; Fogg, D. E. *ACS Catal.* **2015**, *5*, 4690−4698.
(39) Nagarkar, A. A.; Crochet, A.; Fromm, K. M.; Kilbinger, A. F. M. *Macromolecules* **2012**, *45*, 4447−4453.
(40) While binding of tertiary amines such as NEt_3 to Ru centers has been established, the complexes involved are typically less sterically congested arylphosphine derivatives. For a discussion of such complexes and their degradation products, see: (a) Fogg, D. E.; James, B. R. *Inorg. Chem.* **1995**, *34*, 2557−61. For examples of Ru complexes containing macrocyclic, tetradentate tertiary amines, see: (b) Wong, C.-Y.; Lee, F.-W.; Che, C.-M.; Cheng, Y. F.; Phillips, D. L.; Zhu, N. *Inorg. Chem.* **2008**, *47*, 10308−10316 and references therein.
(41) Zhao, Z.-X.; Wang, H.-Y.; Guo, Y.-L. *Rapid Commun. Mass Spectrom.* **2011**, *25*, 3401−3410.
(42) Donor-accelerated methylidene abstraction accounts for the observation of shorter lifetimes for **Ru-4** and related methylidene complexes in THF. See: refs 13, 21. For the methylidene derivative of **Ru-1**, for example, the half-life at 35 °C in THF was 1.1 h, vs 2.5 h in CH_2Cl_2, and 6.6 h in C_6H_6. See: ref 21.
(43) Tomasek, J.; Schatz, J. *Green Chem.* **2013**, *15*, 2317−2338.
(44) Grela, K.; Gulajski, L.; Skowerski, K. Alkene Metathesis in Water. In *Metal-Catalyzed Reactions in Water*; Dixneuf, P. H., Cadierno, V., Eds.; Wiley-VCH: Weinheim, 2013; pp 291−336.
(45) Stark, A.; Ajam, M.; Green, M.; Raubenheimer, H. G.; Ranwell, A.; Ondruschka, B. *Adv. Synth. Catal.* **2006**, *348*, 1934−1941.
(46) Sanford, M. S.; Love, J. A.; Grubbs, R. H. *J. Am. Chem. Soc.* **2001**, *123*, 6543−6554.
(47) Bantreil, X.; Sidi-Ykhlef, M.; Aringhieri, L.; Colacino, E.; Martinez, J.; Lamaty, F. *J. Catal.* **2012**, *294*, 113−118.
(48) Bilel, H.; Hamdi, N.; Zagrouba, F.; Fischmeister, C.; Bruneau, C. *Green Chem.* **2011**, *13*, 1448−1452.
(49) Miao, X.; Fischmeister, C.; Bruneau, C.; Dixneuf, P. H. *ChemSusChem* **2008**, *1*, 813−816.
(50) Alessio, E. *Chem. Rev.* **2004**, *104*, 4203−4242.
(51) Evans, I. P.; Spencer, A.; Wilkinson, G. *J. Chem. Soc., Dalton Trans.* **1973**, 204.
(52) Seddon, E. A.; Seddon, K. R. *The Chemistry of Ruthenium*; Elsevier: Amsterdam, 1984.
(53) Measured rate constants (k_{obs}) for decomposition on reaction with 10 DMSO at 25 °C: for disappearance of **Ru-4a**: 0.003 min^{-1}; for disappearance of **Ru-4a^D**: 0.002 min^{-1} (k_H/k_D = 1.5).
(54) Gomez-Gallego, M.; Sierra, M. A. *Chem. Rev.* **2011**, *111*, 4857−4963.
(55) Ulman, M.; Grubbs, R. H. *J. Org. Chem.* **1999**, *64*, 7202−7207.
(56) Formation of nonlabeled **A**, d_2-**A** and d_3-**A**, in addition to the expected d_1-**A**, may reflect scrambling between the mesityl *o*-CD_3 group, the Ru=CH_2 functionality, and the cyclohexyl rings. Minor scrambling into the cyclohexyl rings is consistent with Figure S10a, while an early report described exchange between the methylidene and cyclohexyl sites in the *d*-labelled first-generation system $RuCl_2(PCy_3)$(=CD_2). See: ref 55. An alternative, intriguing possibility raised by a referee is reversible C−H activation.
(57) Monfette, S.; Eyholzer, M.; Roberge, D. M.; Fogg, D. E. *Chem. - Eur. J.* **2010**, *16*, 11720−11725.
(58) In comparison, use of the second-generation Hoveyda catalyst resulted in 100% conversion in neat toluene or 20:1 toluene−MeCN under the conditions of Table 2, but 31% in 20:1 toluene−H_2O, consistent with Cazin's finding (ref 59) of a more generally deleterious role for water than has hitherto been acknowledged.
(59) Guidone, S.; Songis, O.; Nahra, F.; Cazin, C. S. J. *ACS Catal.* **2015**, *5*, 2697−2701.
(60) Patel, J.; Mujcinovic, S.; Jackson, W. R.; Robinson, A. J.; Serelis, A. K.; Such, C. *Green Chem.* **2006**, *8*, 450−454.
(61) Nickel, A.; Ung, T.; Mkrtumyan, G.; Uy, J.; Lee, C. W.; Stoianova, D.; Papazian, J.; Wei, W.-H.; Mallari, A.; Schrodi, Y.; Pederson, R. L. *Top. Catal.* **2012**, *55*, 518−523.
(62) Vancompernolle, T.; Vignon, P.; Trivelli, X.; Mortreux, A.; Gauvin, R. M. *Catal. Commun.* **2016**, *77*, 75−78.
(63) Arduengo, A. J.; Dias, H. V. R.; Harlow, R. L.; Kline, M. *J. Am. Chem. Soc.* **1992**, *114*, 5530−5534.
(64) van Lierop, B. J.; Reckling, A. M.; Lummiss, J. A. M.; Fogg, D. E. *ChemCatChem* **2012**, *4*, 2020−2025.
(65) Fürstner, A.; Ackermann, L.; Gabor, B.; Goddard, R.; Lehmann, C. W.; Mynott, R.; Stelzer, F.; Thiel, O. R. *Chem. - Eur. J.* **2001**, *7*, 3236−3253.
(66) Lummiss, J. A. M.; Beach, N. J.; Smith, J. C.; Fogg, D. E. *Catal. Sci. Technol.* **2012**, *2*, 1630−1632.
(67) Fürstner, A.; Langemann, K. *Synthesis* **1997**, *1997*, 792−803.
(68) Arduengo, A. J.; Krafczyk, R.; Schmutzler, R.; Craig, H. A.; Goerlich, J. R.; Marshall, W. J.; Unverzagt, M. *Tetrahedron* **1999**, *55*, 14523−14534.
(69) Bailey, G. A.; Fogg, D. E. *ACS Catal.* **2016**, *6*, 4962−4971.

DOI: 10.1021/jacs.6b08372
J. Am. Chem. Soc. 2016, 138, 14668−14677